Directed acyclic decomposition of Kuramoto equations*

Tianran Chen†

Abstract. The Kuramoto model is one of the most widely studied model for describing synchronization behaviors in a network of coupled oscillators, and it has found a wide range of applications. Finding all possible frequency synchronization configurations in a general non-uniform heterogeneous sparse network is an important yet difficult problem due to the complicated nonlinear interactions. In this paper, we develop a general framework for decomposing a Kuramoto network into smaller directed acyclic subnetworks that will form the foundation of a divide-and-conquer approach for studying the frequency synchronization configurations of large Kuramoto networks.

Key words. synchronization, Kuramoto equations, adjacency polytope, polyhedral homotopy

AMS subject classifications. 14Q99, 52B20, 65H10

1. Introduction.

The mathematical modeling and analysis of spontaneous synchronization has found many important applications in physics, chemistry, engineering, biology, and medical science [10]. Originally introduced to describe chemical oscillators, the Kuramoto model [14, 15] became one of the most widely studied model for describing synchronization behaviors in a wide range of different contexts. This paper focuses on the study of frequency synchronization which is a particular type of synchronization behavior where oscillators are tuned into the same frequency. Understanding the set of *all* possible frequency synchronization configurations is the central question here. By choosing an appropriate frame of reference, it is equivalent to the study of the full set of solutions of the system of nonlinear equations

$$\omega_i - \sum_{j\in\mathcal{N}_G(i)} k_{ij}\sin(\theta_i-\theta_j) \;=\; 0 \quad \text{for } i=1,\dots,n.$$

The main contribution of this paper is a general framework for decomposing a Kuramoto network into subnetworks that can be studied more easily. Using a complex algebraic formulation, we can form a continuous deformation of the synchronization equations under which the synchronization configurations degenerates into a union of those of simpler subnetworks supported by directed acyclic subgraphs. By extending our domain to complex phase angles, we can form a new rational system that also captures the synchronization configurations as solutions. This procedure, detailed in section 3, allows the introduction of powerful tools from algebraic geometry. The main ideas is briefly illustrated via a simple example in section 4. Then in section 5, through an abstract construction known as *adjacency polytope* we establish a decomposition of the Kuramoto network into simpler subnetworks induced by facets of this polytope. Each such "facet subnetwork" corresponds to a directed acyclic subgraph of the

*Submitted to the editors DATE.

Funding: This work was funded in part by the AMS-Simons Travel Grant and a Auburn University at Montgomery Grant-In-Aid program.

†Department of Mathematics and Computer Science, Auburn University at Montgomery, Montgomery, Alabama USA (ti@nranchen.org, www.tianranchen.org).

original network. We also explore the topological properties of these subnetworks. The set of these "facet subnetworks" preserves and reveals many important properties of the original network. We show in Theorem 5.7 that the number of synchronization configurations that the original network has is bounded above by the total root count of all the facet subnetworks. In Theorem 5.8 we demonstrate that this decomposition of a network into facet subnetworks can be understood as a a smooth deformation of the synchronization equations that will degenerate into the facet subsystems. Among the possible facet subnetworks, we identify and study the simplest type known as "primitive subnetwork" in section 6. Each primitive subnetwork has a unique synchronization configuration, and hence they form the basic building blocks in such decomposition. Finally we illustrate this decomposition scheme via concrete examples in section 7 and conclude with section 8.

2. Kuramoto model. The Kuramoto model [14] is a mathematical model for studying behavior of a network of coupled oscillators. Here an oscillator is simply an object that can continuously vary between two states. In isolation, each oscillator has its own natural frequency. When we consider networks of coupled oscillators, however, rich and complex dynamic behaviors start to appear. The oscillators are coupled with one another by idealized springs whose stiffness are characterized by their *coupling strength*: For a pair of oscillators (i, j), the real number k_{ij} quantifies the strength of coupling between them. The topology of a network of $N = n + 1$ oscillators is modeled by a graph $G = (V, E)$ in which nodes $V = \{0, \dots, n\}$ represent the oscillators and the edges E represent their connections. The coupling strengths $K = \{k_{ij}\}$ and the natural frequencies $\omega = (\omega_0, \dots, \omega_n)$ captures the quantitative information of the network. In its simplest form, the Kuramoto model is a differential equation that describes the nonlinear interactions in such a network given by

$$\dot{\theta}_i(t) \;=\; \omega_i - \sum_{j \in \mathcal{N}_G(i)} k_{ij} \sin(\theta_i(t) - \theta_j(t)) \quad \text{for } i = 0, \dots, n \text{ and } t \geq 0 \tag{2.1}$$

where $\mathcal{N}_G(i)$ denotes the neighbors of node i, and its state is represented by its phase angle $\theta_i(t)$ as a function time t. The network described by (G, K, ω) together with the above differential equation will be referred to as a **Kuramoto network**. Central to this paper are the special configurations in which the angular velocity of all oscillators become perfectly aligned, known as **frequency synchronization configurations**. That is, $\frac{d\theta_i}{dt} = c$ for $i = 0, \dots, n$ and a constant c. By adopting a proper frame of reference, we can assume $c = 0$, and the (frequency) synchronization configurations are simply equilibria of the Kuramoto model (2.1) given by

$$\omega_i - \sum_{(i,j) \in \mathcal{N}_G(i)} k_{ij} \sin(\theta_i(t) - \theta_j(t)) \;=\; 0 \quad \text{for } i = 0, \dots, n \text{ and } t \geq 0. \tag{2.2}$$

To remove the inherent degree of freedome induced by uniform translation, the standard practice is to choose node 0 to be the *reference node* and set $\theta_0 = 0$. Assuming the coupling strength are symmetric, i.e., $k_{ij} = k_{ji}$, the $n + 1$ equations are then linearly dependent which allows one equation to be eliminated, producing a system of n equations in n unknowns $\theta_1, \dots, \theta_n$. This **synchronization system** is the main focus of this paper, and the key question we set out to answer is whether or not the full set of solutions to this system can be understood by studying simpler subnetworks of the original Kuramoto network.

3. Complex algebraic formulation of the synchronization equations. Even though the original formulation of the synchronization equations (2.2) considers only real phase angles, it is useful to expand the domain to the more general complex phase angles as this would allow us to apply powerful tools from complex algebraic geometry. Consider complex phase angle $z_i = \theta_i - r_i\mathbf{i}$ for $i = 0, \ldots, n$ where $\mathbf{i} = \sqrt{-1}$. Using the identity $\sin(z) = \frac{1}{2\mathbf{i}}(e^{\mathbf{i}z} - e^{-\mathbf{i}z})$ we define the new complex variable

$$x_i = e^{\mathbf{i}z_i} = e^{r_i+\mathbf{i}\theta_i} \quad \text{for } i = 1, \ldots, 0 \quad \text{and } x_0 = e^{0+0\mathbf{i}} = 1. \tag{3.1}$$

They represent the phases of the oscillator as points on the complex plane. If $r_i = 0$, then x_i lies on the unit circle as the original formulation requires. If $r_i \neq 0$, x_i will deviate from the unit circle and no longer represent solutions of the original equations. Such *extraneous solutions* (i.e. non-real solutions), however, can be identified easily. With these new variables, the transcendental terms in (2.2) can be converted to rational functions

$$\sin(z_i - z_j) = \frac{e^{z_i\mathbf{i}}e^{-z_j\mathbf{i}} - e^{z_j\mathbf{i}}e^{-z_i\mathbf{i}}}{2\mathbf{i}} = \frac{1}{2\mathbf{i}}\left(\frac{x_i}{x_j} - \frac{x_j}{x_i}\right),$$

and the system (2.2) is transformed into the **algebraic synchronization system**

$$\omega_i - \sum_{(i,j)\in\mathcal{N}_G(i)} a'_{ij}\left(\frac{x_i}{x_j} - \frac{x_j}{x_i}\right) = 0 \quad \text{for } i = 1, \ldots, n \tag{3.2}$$

in the complex variables $x_1, \ldots, x_n$ where $a'_{ij} = \frac{k_{ij}}{2\mathbf{i}}$. Naturally, in this formulation, we also allow complex coupling strength and natural frequencies. This algebraic formulation has been used in [3, 5], and it is similar to the formulation in [2]. However, the above formulation directly connects to the construction of "adjacency polytopes".

Denote the rational functions on the left hand side of the above system by $\mathbf{f} = (f_1, \ldots, f_n)^\top$. It is clear that the two systems $\mathbf{f} = \mathbf{0}$ and $M\mathbf{f} = \mathbf{0}$ have the exact same solution set for any nonsingular $n \times n$ matrix $M = [M_{ij}]$. Therefore, without loss, we can consider the equivalent system $M\mathbf{f} = \mathbf{0}$ which is of the form

$$c_k - \sum_{(i,j)\in\mathcal{E}(G)} a_{ijk}\left(\frac{x_i}{x_j} - \frac{x_j}{x_i}\right) = 0 \quad \text{for } k = 1, \ldots, n \tag{3.3}$$

with $c_k = \sum_{i=1}^n M_{ki}\omega_i$. This system will be referred to as the **unmixed form** of the algebraic synchronization system (simply **unmixed synchronization system** hereafter). Replacing a system of equations $\mathbf{f} = \mathbf{0}$ by $M\mathbf{f} = \mathbf{0}$ for a nonsingular square matrix M is a common practice in numerical methods for solving nonlinear systems (e.g., the *randomization* procedure in numerical algebraic geometry [18]).

In this form, every monomial appears in every equation, and each equation no longer represents the balancing condition on a single oscillator, instead it is a linear combination of all balancing conditions in the network. The rest of the paper will focus on this system.

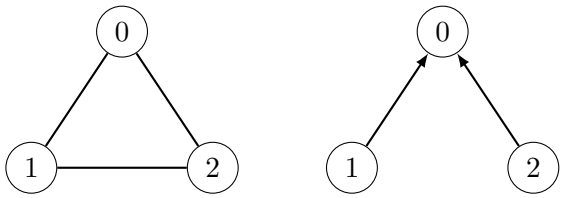

(a) 3 coupled oscillators (b) A subnetwork of (a)

Figure 1. *A network of 3 coupled oscillators and one of its subnetwork*

4. A example. Here, we briefly outline the basic idea behind the proposed decomposition scheme via the simple example of a network of 3 coupled oscillators shown in Figure 1a. Even though this case is simple enough to be solved directly by algebraic manipulations, it will still provide an illuminating glimpse to the main idea of the proposed framework. In this case, the unmixed synchronization system (3.3) is

$$\begin{cases} c_1 - \left[a_{101}(x_1x_0^{-1} - x_1^{-1}x_0) + a_{121}(x_1x_2^{-1} - x_1^{-1}x_2) + a_{201}(x_2x_0^{-1} - x_2^{-1}x_0)\right] = 0 \\ c_2 - \left[a_{102}(x_1x_0^{-1} - x_1^{-1}x_0) + a_{122}(x_1x_2^{-1} - x_1^{-1}x_2) + a_{202}(x_2x_0^{-1} - x_2^{-1}x_0)\right] = 0. \end{cases} \tag{4.1}$$

The root count results developed in [5] and [2] both state that, there are no more than 6 complex synchronization configurations for this Kuramoto network of 3 oscillators. The goal here is to understand these synchronization configurations by examining simpler subnetworks of this network.

Figure 2 shows the proposed decomposition of this Kuramoto network into 6 subnetworks supported by directed acyclic graphs (i.e. with asymmetric couplings) with each subnetwork correspond to one of the possible complex synchronization configuration.

Each of the subnetworks has its own synchronization equations. For instance, the subnetwork shown in Figure 1b has the unmixed synchronization system given by

$$\begin{aligned} c_1 &= a_{110}x_1/x_0 + a_{120}x_2/x_0 \\ c_2 &= a_{210}x_1/x_0 + a_{220}x_2/x_0 \end{aligned}$$

which is a system of equations involving a subset of terms in (4.1). Here, each edge is interpreted as a directed edge, and the directed edge (i, j) corresponds to the term x_i/x_j. It is easy to verify that for generic choices of the coefficients, the above system has a unique complex solutions. The same analysis can be applied to rest of the subnetworks shown in Figure 2, and we can verify that the synchronization system induced by each subnetwork has a unique solution under the assumption of generic coefficients. Moreover, these solutions are in one-to-one correspondence with the 6 complex frequency synchronization configurations of the original network in Figure 1a via a homotopy function given by

$$H(x_1, x_2, t)\begin{cases} \dfrac{\omega_1}{t} - \left[a_{101}\left(\dfrac{x_1}{x_0} - \dfrac{x_0}{x_1}\right) + a_{121}\left(\dfrac{x_1}{x_2} - \dfrac{x_2}{x_1}\right) + a_{201}\left(\dfrac{x_2}{x_0} - \dfrac{x_0}{x_2}\right)\right] \\ \dfrac{\omega_2}{t} - \left[a_{102}\left(\dfrac{x_1}{x_0} - \dfrac{x_0}{x_1}\right) + a_{122}\left(\dfrac{x_1}{x_2} - \dfrac{x_2}{x_1}\right) + a_{202}\left(\dfrac{x_2}{x_0} - \dfrac{x_0}{x_2}\right)\right] \end{cases}.$$

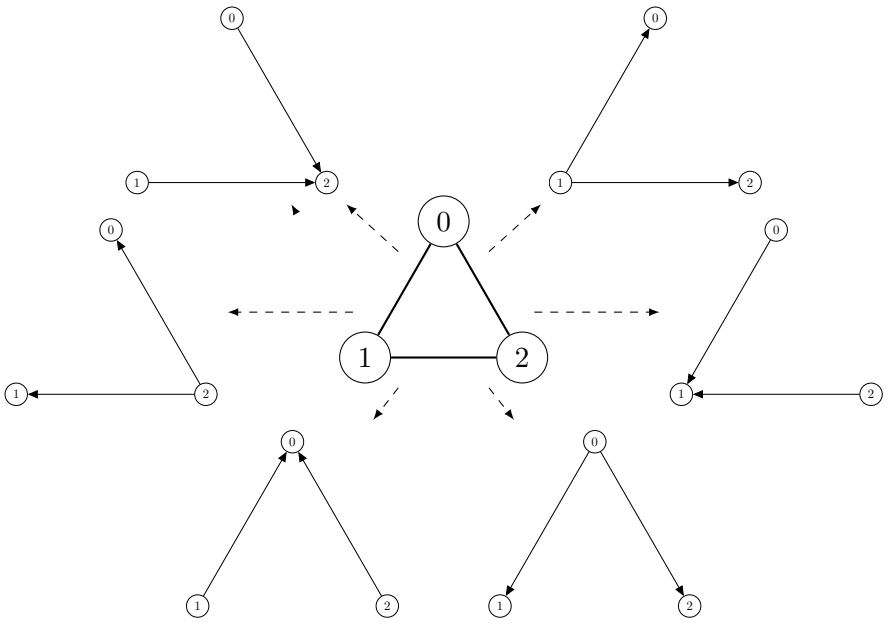

Figure 2. *A decomposition of a network of 3 oscillators (center) into 6 subnetworks supported by directed acyclic graphs.*

Clearly, at $t = 1$, the equation $H(x_1, x_2, 1) = 0$ is equivalent to the original unmixed synchronization system (4.1). Under a mild "genericity" assumption, it can be shown that as t varies continuously from 1 toward 0 (without reaching 0), the complex solutions of $H(x_1, x_2, t) = 0$ also move smoothly forming smooth paths emanating from the solutions at $t = 1$.

As t approaches 0, H becomes undefined, and the 6 solution paths degenerate into the complex frequency synchronizations configurations of the 6 subnetworks show in Figure 1a in the sense that the 6 complex synchronization configurations of the 6 subnetworks are the limit points of the following reparametrization of the 6 paths:

$$\begin{array}{cccccc} x_1 = y_1 & x_1/t = y_1 & x_1/t = y_1 & x_1 = y_1 & x_1 t = y_1 & x_1 t = y_1 \\ x_2 t = y_2 & x_2/t = y_2 & x_2 = y_2 & x_2/t = y_2 & x_2 = y_2 & x_2 t = y_2. \end{array}$$

That is, as $t \to 0$, along each path, (y_1, y_2) converge to the unique solution of the synchronization systems of one of the subnetworks shown in the decomposition Figure 2.

5. Adjacency polytope and facet decomposition. The decomposition illustrated above is constructed from the geometric information encoded in a polytope — the adjacency polytope. The construction of adjacency polytopes in the context of Kuramoto models is studied in detail in [3] and [5]. Here we briefly review the definition. A polytope is the convex hull of a finite lists of points in $\mathbb{R}^n$ (a bounded geometric object with finitely many flat faces). The adjacency polytope is a polytope that will capture the topological information of the Kuramoto network, provide a bound on the number of synchronization configurations, and guide us in the decomposition of the network.

Definition 5.1 ([3]). *Given a Kuramoto network (G, K, ω), the* ***adjacency polytope*** *of this network is the polytope*

$$\nabla_G = \operatorname{conv}\{\mathbf{e}_i - \mathbf{e}_j \mid (i,j) \in \mathcal{E}(G)\}, \tag{5.1}$$

and the ***adjacency polytope bound*** *of this network is the* normalized volume[1] $\operatorname{NVol}(\nabla_G)$.

Here $\mathbf{e}_i$ is the i-th standard basis of $\mathbb{R}^n$ and $\mathbf{e}_0 = \mathbf{0}$. The adjacency polytope is the convex hull of entries in the (directed) adjacency list of the graph as points in $\mathbb{R}^n$, and it can be considered as a geometric encoding of the network topology of the network. In the context of Kuramoto model and the closely related problem of power flow equations, this concept was first developed in [3] and [7] respectively. In [3], it is shown that the adjacency polytope bound is a sharp upper bound for the total number of isolated complex synchronization configurations for certain graphs. This upper bound is sharp in the sense that it is attainable when generic coupling strength and natural frequencies are used. The explicit formula for this upper bound in the case of cycle graphs and tree graphs are established in [5].

5.1. Facet subnetworks and subsystems. The main goal of this paper is to show much more information of the original Kuramoto network can be extracted from this polytope. Indeed, each facet of the adjacency polytope gives rise to a directed acyclic subnetwork of the original network. To define such generalized Kuramoto networks, we first need to reinterpret the synchronization equations (3.2) and (3.3) from the view point of directed graphs. In (3.2), an (undirected) edge $\{i, j\}$ corresponds to the term $a'_{ij}(x_i/x_j - x_j/x_i)$. We split this undirected edge into directed edges (i, j) and (j, i) with the corresponding terms $a'_{ij}x_i/x_j$ and $a'_{ij}x_j/x_i$ respectively as shown in Figure 3. This allows us to define more general directed Kuramoto networks induced by special directed graphs:

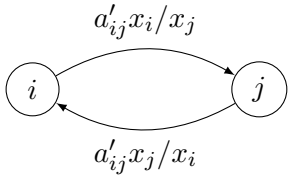

Figure 3. *Two directed edges*

Definition 5.2. *For a facet F of the adjacency polytope ∇_G, we define*

$$\mathcal{V}_F = \{i \mid \mathbf{e}_i - \mathbf{e}_j \in F \text{ or } \mathbf{e}_j - \mathbf{e}_i \in F \text{ for some } j\}$$
$$\mathcal{E}_F = \{(i,j) \mid \mathbf{e}_i - \mathbf{e}_j \in F\}.$$

With these, we define the ***facet subnetwork*** *associated with F to be the (asymmetric) Kuramoto network $(\mathcal{V}_F, \mathcal{E}_F)$ and the corresponding* ***facet subsystem*** *to be the system of equations*

$$c_k - \sum_{(i,j)\in\mathcal{E}_F} a_{kij}\left(\frac{x_i}{x_j}\right) = 0 \quad \text{for each } k \in \mathcal{V}_F. \tag{5.2}$$

The facet subsystem is a system of equations involving a subset of terms in the unmixed synchronization system (3.3) of the original network. The selection of the terms depends on the nodes and edges appears in the corresponding facet network. Here we consider the edge (i, j) to be an directed edge. That is, $(i, j) \in \mathcal{E}_F$ does not imply $(j, i) \in \mathcal{E}_F$. Indeed, as we shall prove, the directed edges (i, j) and (j, i) can never be in the same facet subnetwork.

[1]The normalized the volume of a d-dimensional lattice polytope in $\mathbb{R}^d$ is the product of its volume and $d!$. It is easy to verify that this normalized volume is always an integer.

Remark 5.3. The splitting of an undirected edge into two directed edges shown in Figure 3 can also be interpreted as an explicit use of an imaginary interaction term. In considering real frequency synchronization configurations defined by (2.2), we require $|x_i| = 1$ for $i = 1, \dots, n$ since $x_i = e^{r_i + \mathbf{i}\theta_i}$. In this case,

$$a'_{ij}\frac{x_i}{x_j} = \frac{k_{ij}}{2\mathbf{i}}e^{\mathbf{i}(\theta_i - \theta_j)} = \frac{k_{ij}}{2}[\sin(\theta_i - \theta_j) - \mathbf{i}\cos(\theta_i - \theta_j)]$$

which can be interpreted as the interaction term along the directed edge (i, j). If both (i, j) and (j, i) are present, then the imaginary parts cancel leaving only the real part

$$\frac{k_{ij}}{2}[\sin(\theta_i - \theta_j) - \mathbf{i}\cos(\theta_i - \theta_j)] - \frac{k_{ij}}{2}[\sin(\theta_j - \theta_i) - \mathbf{i}\cos(\theta_j - \theta_i)] = k_{ij}\sin(\theta_i - \theta_j)$$

as the combined interaction term which matches the original synchronization equations (2.2). This interpretation of the unidirectional interaction is similar to that used in the recent studies in Kuramoto models on directed graphs (e.g. [9]).

5.2. Topological properties of facet subnetworks. A natural question to ask here is what special topological properties do facet subnetworks posses? We can verify that the special construction imposes certain topological restriction and limit the number of edges.

Theorem 5.4. *Given a Kuramoto network, let ∇_G be its adjacency polytope. Then for each facet F of ∇_G, the facet system (5.2) is a synchronization system supported by a Kuramoto subnetwork whose underlying directed graph G_F has the following properties:*

- *acyclic;*
- *contains all the nodes of G;*
- *all paths between a pair of nodes have the same length; and*
- *each paths in G_F contains no more than half of the edges of any undirected cycle in G containing it.*

Proof. Let $\boldsymbol{\alpha} = (\alpha_1, \dots, \alpha_n) \in \mathbb{R}^n$ be the inner normal vector of the facet F of ∇_G, then there exists an $h \in \mathbb{R}$ such that

$$\begin{aligned} \langle \mathbf{p}, \alpha \rangle &= h \quad \text{for all } \mathbf{p} \in F \text{ while} \\ \langle \mathbf{p}, \alpha \rangle &> h \quad \text{for all } \mathbf{p} \in \nabla_G \setminus F. \end{aligned}$$

But $\mathbf{0}$ is an interior point of ∇_G, therefore

$$h < \langle \mathbf{0}, \alpha \rangle = 0.$$

(Acyclic) Suppose G_F contains a directed cycle $i_1 \to i_2 \to \cdots \to i_m \to i_1$ for some nonempty set of oscillators $\{i_1, \dots, i_m\} \subset \{0, \dots, n\}$. Define $i_{m+1} = i_1$, then $\mathbf{e}_{i_k} - \mathbf{e}_{i_{k+1}} \in F$ for each $k = 1, \dots, m$. Since $\boldsymbol{\alpha}$ is the inner normal vector of F, we have

$$\left\langle \mathbf{e}_{i_k} - \mathbf{e}_{i_{k+1}}, \boldsymbol{\alpha} \right\rangle = \alpha_{i_k} - \alpha_{i_{k+1}} = h < 0 \quad \text{for each } k = 1, \dots, m,$$

and hence

$$\alpha_{i_1} < \alpha_{i_2} < \cdots < \alpha_{i_m} < \alpha_{i_1},$$

which is a contradiction. Therefore G_F cannot contain any directed cycles.

(Containing all nodes) For the cases with $n = 1$, there are exactly two directed edges, and they correspond to the two facets of the polytope ∇_G which is simply a line segment. The statement is clearly in these cases.

For $n > 1$, since $\dim \nabla_G = n$, the facet F of ∇_G thus has dimension $n-1$. Suppose there is a node $i \notin G_F$. Without loss of generality, by reassigning the reference node, we can assume $i \neq 0$. Let G' be the graph obtained from G by removing the node i and all edges associated with it. Then $\nabla_{G'} \subset \nabla_G$, and the set of vertices of $\nabla_{G'}$ is a subset of the vertices of ∇_G. It is straightforward to verify that F remains a face of $\nabla_{G'}$. Therefore $\dim F < \dim \nabla_{G'} \leq n-1$ which contradict with the assumption that $\dim F = n-1$. We can thus conclude that G_F contains all the nodes of G.

(Equal length) Suppose there are two paths $i_0 \to i_2 \to \cdots \to i_m$ and $j_0 \to j_2 \to \cdots \to j_\ell$ with the same starting and end points, that is, $i_0 = j_0$ and $i_m = j_\ell$. Then

$$\left\langle \mathbf{e}_{i_k} - \mathbf{e}_{i_{k+1}} , \boldsymbol{\alpha} \right\rangle = h \quad \text{for each } k = 0, \ldots, m-1$$

Summing over these m equations, we obtain

$$\langle \mathbf{e}_{i_0} - \mathbf{e}_{i_m} , \boldsymbol{\alpha} \rangle = mh.$$

Similarly, summing over the ℓ equations along the path $j_0 \to j_2 \to \cdots \to j_\ell$ produces

$$\langle \mathbf{e}_{j_0} - \mathbf{e}_{j_\ell} , \boldsymbol{\alpha} \rangle = \ell h.$$

But $j_0 = i_0$ and $i_m = j_\ell$, thus we must have $mh = \ell h$, i.e., $m = \ell$, and these two paths must have the same length.

(Half cycle) Suppose G contains an undirected cycle $i_0 \leftrightarrow \cdots \leftrightarrow i_m \leftrightarrow \cdots \leftrightarrow i_\ell = i_0$. Among these edges, the path $i_0 \to i_2 \to \cdots \to i_m$ is in G_F we shall show m is no more than $\ell/2$. By construction, $\mathbf{e}_{i_k} - \mathbf{e}_{i_{k+1}} \in F$ for each $k = 0, \ldots, m-1$, and hence

$$\left\langle \mathbf{e}_{i_k} - \mathbf{e}_{i_{k+1}} , \boldsymbol{\alpha} \right\rangle = h \quad \text{for each } k = 0, \ldots, m-1.$$

Summing over these m equations, we obtain

$$\langle \mathbf{e}_{i_1} - \mathbf{e}_{i_m} , \boldsymbol{\alpha} \rangle = mh.$$

Similarly, consider the path $i_\ell \to i_{\ell-1} \to \cdots \to i_m$ which is in G, we must have

$$\left\langle \mathbf{e}_{i_{k+1}} - \mathbf{e}_{i_k} , \boldsymbol{\alpha} \right\rangle \geq h \quad \text{for each } k = m, \ldots, \ell-1.$$

Summing over these equations produces

$$\langle \mathbf{e}_{i_1} - \mathbf{e}_{i_m} , \boldsymbol{\alpha} \rangle \geq (\ell - m)h$$

Recall that $\langle \mathbf{e}_{i_1} - \mathbf{e}_{i_m} , \boldsymbol{\alpha} \rangle = mh$, so we must have $mh \geq (\ell - m)h$. Since $h < 0$, this implies that $m \leq \ell - m$, i.e., $2m \leq \ell$. ∎

5.3. Algebraic properties of facet subsystems. A fundamental fact in complex algebraic geometry is that, as far as complex root count is concerned, the generic behavior of a family of algebraic systems coincides with the maximal behavior. That is, if we consider the facet system as a family of algebraic systems parametrized by the coefficients, then the generic complex root count coincide with the maximum root count. Applying this to our context, we obtain the following proposition.

Proposition 5.5. *For a generic choice of the coefficients $\{c_k\}$ and $\{a_{ijk}\}$, the total number of isolated*[2] *complex solutions to a given facet subsystem (5.2) induced by the facet F of an adjacency polytope is a constant. Denote this constant by $\mathcal{N}(F)$, then $\mathcal{N}(F)$ is also the maximum number of isolated complex solutions this facet subsystem could have.*

This proposition can be understood as a direct application of the cheater's homotopy [16] or the parameter homotopy [17] theory to the facet subsystems. Moreover, Kushnirenko's Theorem [13] provides us the explicit formula for the maximum root count in the form of normalized volume.

Proposition 5.6. *Let F be a facet of the adjacency polytope $P(G)$, then*

$$\mathcal{N}(F) = \mathrm{NVol}(\mathrm{conv}(F \cup \{\mathbf{0}\})).$$

Proof. Since the directed graph $(\mathcal{V}_F, \mathcal{E}_F)$ associated with a facet subnetwork is necessarily acyclic by Theorem 5.4, the edges (i, j) and (j, i) cannot both be in $\mathcal{E}_F$. Consequently, the coefficients in the facet subsystem (5.2) are independent. That is, generic choices of the parameters $\{c_k\}$ and $\{a_{ijk}\}$ for network correspond to independent generic choices of the coefficients for the facet subsystem.

Also note that the *support* of the facet subsystem — the collection of all the exponent vectors appeared in the system — is precisely the the vertices of F together with $\mathbf{0}$. By Kushnirenko's Theorem [13], $\mathcal{N}(F) = \mathrm{NVol}(\mathrm{conv}(F \cup \{\mathbf{0}\}))$. ∎

$\mathcal{N}(F)$ can be considered as a generalization of the adjacency polytope bound to facet subnetworks. Moreover, the sum of the root count for *all* facet subsystems gives us a root count for the whole system.

Theorem 5.7. *Given a Kuramoto network, let ∇_G be the adjacency polytope defined above. Then the total number of isolated complex synchronization configurations this network has is bounded above by the sum of generic complex root counts of the facet subsystems, that is, it is bounded by*

$$\sum_{F \in \mathcal{F}(\nabla_G)} \mathcal{N}(F)$$

where $\mathcal{F}(\nabla_G)$ is the set of facets of the polytope ∇_G.

Proof. $\mathbf{0}$ is an interior point of ∇_G. Thus the collection of pyramids

$$\{\mathrm{conv}(F \cup \{\mathbf{0}\}) \mid F \in \mathcal{F}(\nabla_G)\}$$

[2] Isolated solutions here refer to geometrically isolated solutions. A solution of a system of equations is said to be geometrically isolated if there is a nonempty open set in which it is the only solution.

form a subdivision of ∇_G. Therefore the normalized volume of ∇_G is the sum of the normalized volume of these pyramid. That is,

$$\mathrm{NVol}(\nabla_G) = \sum_{F \in \mathcal{F}(\nabla_G)} \mathrm{NVol}(\mathrm{conv}(F \cup \{\mathbf{0}\}))$$

■

Combining this result and Theorem 5.4, it is plausible that the adjacency polytope bound $\mathrm{NVol}(\nabla_G)$ can be computed simply by listing all the possible facet subnetworks and compute the adjacency polytope bound for each of such simpler subnetworks which is potentially easier than the #P problem of volume computation in general. As we will show in the examples in section 7, this can be done for certain classes of networks.

5.4. Degeneration into facet subsystems. The true value of the facet subsystems lies in their roles as destinations for a deformation of the synchronization equations. That is, we can form a continuous deformation (in the sense of homotopy) of the unmixed synchronization equations that will degenerate into the simpler facet subsystems and thereby reduce the problem of finding synchronization configurations to the problem of solving each individual facet subsystems. This is done through a specialized homotopy.

Consider the homotopy $H(\mathbf{x}, t) = (H_1, \ldots, H_k)$ given by

$$H_k(x_1, \ldots, x_n, t) = \frac{c_k}{t} - \sum_{(i,j) \in \mathcal{E}(G)} a_{ijk} \left(\frac{x_i}{x_j} - \frac{x_j}{x_i} \right) \quad \text{for } k = 1, \ldots, n. \tag{5.3}$$

Clearly, the equation $H(\mathbf{x}, 1) = \mathbf{0}$ is exactly the unmixed synchronization system (3.3). Since $H(\mathbf{x}, t)$ is smooth in t for $t \in (0, 1]$, as t vary continuously between 0 and 1, the equation $H(\mathbf{x}, t) = \mathbf{0}$ represents a continuous deformation of (3.3). With proper choices of the coefficients, the solutions of $H(\mathbf{x}, t) = \mathbf{0}$ also move smoothly as t varies within $(0, 1]$ forming smooth *solution paths*. As $t \to 0$, however, this smooth deformation breaks down, and the equation $H(\mathbf{x}, t) = \mathbf{0}$ degenerates into the facet subsystems.

Theorem 5.8. *Given a Kuramoto network (G, K, ω) with generic coupling strengths and natural frequencies, consider the homotopy $H(\mathbf{x}, t)$ defined above. The solution set of the system of equations $H(\mathbf{x}, t) = \mathbf{0}$ contains a finite number of smooth curves parametrized by t such that*

1. *the set of limit points of these curves as $t \to 1$ contains all isolated complex synchronization configurations of this network; and*
2. *the set of limit points of these curves as $t \to 0$ reaches all the complex synchronization configurations of the facet subsystems at "toric infinity" in the sense that for each of these complex solutions $\mathbf{y} = (y_1, \ldots, y_n)$, there exists a curve defined by $H(\mathbf{x}, t) = \mathbf{0}$ along which $x_i(t) = y_i t^{\alpha_i} + o(t)$ for some $\alpha_i \in \mathbb{Q}$ and t sufficiently close to 0.*

Proof. (1) This statement is a directed consequence of the parameter homotopy method [17]. If we consider the unmixed synchronization system (3.3) as a family $\mathbf{f}(\mathbf{x}; \mathbf{c})$ of nonlinear systems parametrized by the constant terms $\mathbf{c} = (c_1, \ldots, c_n)$, then by choosing a generic $\mathbf{c}$, for every $t \in (0, 1]$, the parameter $\mathbf{c}/t$ remains generic. By the theory of parameter homotopy [17], the solution set of $H(\mathbf{x}, t) = \mathbf{0}$ in $\mathbb{C}^n \times (0, 1]$ consists of smooth paths parametrized by t whose limit points as $t \to 1$ include all solutions of $H(\mathbf{x}, 1) \equiv \mathbf{f}(\mathbf{x}; \mathbf{c}) = \mathbf{0}$.

(2) Let $C \subset \mathbb{C}^n \times (0,1]$ be a curve defined by $H(\mathbf{x},t) = \mathbf{0}$, then by the previous part, C can be expressed as a path $\mathbf{x}(t)$ smoothly parametrized by t (i.e., $\mathbf{x}$ is differentiable in t for $t \in (0,1]$ and holomorphic in t, as a complex variable for t in a sufficiently small punctured disk centered at 0) for $t \neq 0$. Though the smoothness breaks down at $t = 0$, by the theory of polyhedral homotopy method [12] as well as Newton-Puiseux Theorem, there exists a smooth function $\mathbf{y}(t) = (y_1, \ldots, y_n)$ and a vector $\boldsymbol{\alpha} = (\alpha_1, \ldots, \alpha_n) \in \mathbb{Q}^n$ such that $\mathbf{y}(t)$ has a limit point in $\mathbb{C}^n$ as $t \to 0^+$ and

$$\mathbf{x}(t) = \mathbf{y}(t) \cdot t^{\boldsymbol{\alpha}} = (y_1(t)\, t^{\alpha_1}, \cdots, y_n(t)\, t^{\alpha_n})$$

for sufficiently small $t > 0$. Moreover, $\hat{\boldsymbol{\alpha}} = (\boldsymbol{\alpha}, 1) \in \mathbb{Q}^{n+1}$ must be an inner normal vector of a facet of the Newton polytope of $H(\mathbf{x},t)$ which is the pyramid formed by $\nabla_G \subset \mathbb{R}^n \subset \mathbb{R}^{n+1}$ together with $(\mathbf{0}, -1) \in \mathbb{R}^{n+1}$, i.e., $\hat{\boldsymbol{\alpha}}$ is an inner normal vector of

$$\operatorname{Newt}(H) = \operatorname{conv}\left(\{(\mathbf{x}, 0) \mid \mathbf{x} \in \nabla_G\} \cup \{(\mathbf{0}, -1)\}\right).$$

Then $\boldsymbol{\alpha}$ is an inner normal vector of a facet F of ∇_G. Consequently, the initial form $\operatorname{init}_\alpha(H)$ is exactly the facet subsystem induced by F as shown in (5.2), and $\lim_{t\to 0^+} \mathbf{y}$ is a solution to this system. ∎

The above theorem reduces the problem of solving a complicated synchronization system (3.3) to the problem of solving the simpler facet subsystems: Once the solutions of each facet subsystem are found, they become the starting points of the smooth paths defined by $H(\mathbf{x},t) = \mathbf{0}$, and standard numerical "path tracking" algorithms [1, 6, 8, 18] can then be applied to follow these smooth paths and reach the desired synchronization configurations defined by $H(\mathbf{x}, 1) = \mathbf{f}(\mathbf{x}) = \mathbf{0}$.

Remark 5.9. The homotopy constructed from the above theorem can be viewed as a highly specialized polyhedral homotopy method [12] with the special lifting function that takes the value of -1 on the constant terms and zero everywhere else. Moreover, instead of degenerate into binomial systems that depends on liftings, our homotopy degenerate into facet subsystems that can be found by examining network topology.

6. Primitive directed acyclic Kuramoto system.

The general facet decomposition scheme outlined above decomposes a Kuramoto network into a collection of smaller directed acyclic networks involving the original oscillators. Among these subnetworks, the basic building blocks are "primitive" subnetworks which are, in a sense, the smallest Kuramoto networks that could have a frequency synchronization configuration.

Definition 6.1. *A subnetwork is called* ***primitive*** *if the underlying graph G is a connected acyclic graph that contains all the vertices $0, \ldots, n$ and exactly $n = N - 1$ directed edges.*

Since such a primitive subnetwork contains exactly N node and $N - 1$ directed edges. Removing any edge will create disconnected components. It is thus a minimum subnetwork in that sense. Yet, as we shall show, it is sophisticated enough to have a complex synchronization configuration, and this configuration *must be unique*. Equally importantly, this unique synchronization configuration can be *computed quickly and easily* using only $O(n)$ multiplications and divisions and no additional memory.

Theorem 6.2. *The facet subsystem* (5.2) *supported by a primitive facet subnetwork has a* unique *complex solution.*

Proof. Since G has exactly n directed edges, the corresponding synchronization system has exactly n nonconstant terms in each equation. Under the assumption of generic coefficients, we can reduce the system to

$$c'_k = a'_k x_{i_k}/x_{j_k} \quad \text{for } k = 1, \ldots, n.$$

via Gaussian elimination with no cancellation of the terms with $\{c'_k\}$ and $\{a'_k\}$ representing the resulting coefficients. Having exactly $n = N - 1$ edges and N nodes also ensures that the underlying undirected graph is an undirected tree. Therefore for each $i = 1, \ldots, n$, there is a unique path between node 0 and node i through the nodes $i_0, i_1, \ldots, i_m$ with $i_0 = 0$ and $i_m = i$ where m is the length of this path.

$$\begin{aligned} c'_1 &= a'_1 x_{i_1}^{\pm 1} x_{i_0}^{\mp 1} \\ c'_2 &= a'_2 x_{i_2}^{\pm 1} x_{i_1}^{\mp 1} \\ &\vdots \\ c'_m &= a'_m x_{i_m}^{\pm 1} x_{i_{m-1}}^{\mp 1}. \end{aligned}$$

Recall that node 0 is the reference node, i.e., $x_{i_0} = x_0 = 1$. Solving this system via a forward substitution process, we can determine the value of $x_{i_m} = x_i$. Since the path between the node i and node 0 is unique, there is no possibility of inconsistency in this process, and hence the value of each x_i is uniquely determined. We can therefore conclude that a solution to the facet system exists, and it is unique. ∎

Remark 6.3. From a computational view point, the true value of primitive subnetworks lies in the ease with which it can be solved. The above proof is constructive and suggests a practical algorithm for solving the facet subsystem that only require $O(n)$ complex multiplication and divisions and no additional memory. This is of great importance in the homotopy method for solving the synchronization system described in the previous section since the solutions to the facet subsystems are the starting points of solutions paths that will lead to the desired synchronization configurations of the original Kuramoto network.

Remark 6.4. The above theorem can also be interpreted in the language of toric algebraic geometry as follows. The facet subsystem supported by a primitive facet subnetwork can be reduced to an equivalent binomial system whose associated exponent matrix (the matrix whose columns are the exponent vectors for the nonconstant terms) is a unimodular matrix. Consequently, it defines a (normal) irreducible toric variety of zero dimension which must be a single point. From this view point, we can also see that primitive subnetworks are the smallest building blocks in the sense of toric geometry.

As the next section will demonstrate, primitive subnetworks appear naturally in the facet decomposition of many types of Kuramoto networks, e.g., trees, cycles, and chordal graphs. Indeed, in some cases, all facet subnetworks are primitive.

7. Examples. In this section, we illustrate the facet decomposition scheme via concrete examples. In all examples, the facets of the adjacency polytopes are computed using the software package Polymake [11].

7.1. Tree graphs. For a tree graph containing 5 nodes shown in Figure 4, the corresponding adjacency polytope (Definition 5.1) has 16 facets which produces 16 facet subnetworks shown in Figure 5. *Every facet subnetwork is primitive in this case.* Since each primitive facet subnetwork has a unique complex synchronization configuration, we can conclude that the original tree network has at most 16 complex synchronization configurations. This coincide with the well known result that on a tree network of N oscillators, there are at most 2^{N-1} complex synchronization configurations. Indeed, this facet decomposition scheme actually reproduced the tightest possible upper bound on the number of *real* synchronization configurations as it is known that there could also be as many as 2^{N-1} real synchronization configurations [2]. Note that in this case, the topological constraints given in Theorem 5.4 actually determines the list of facet subnetworks. That is, without actually computing the facets of the adjacency polytope, one can easily enumerate all the facet subnetworks by listing all acyclic subgraphs.

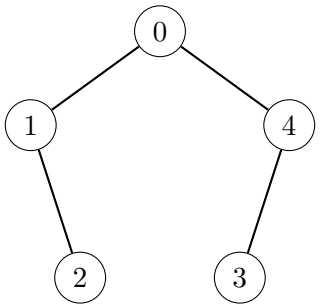

Figure 4. *A tree of 5 nodes*

7.2. Cycle graphs. Figure 7 shows all the facet subnetworks from a cycle graph of 5 nodes (Figure 6). Each subnetwork is primitive and hence has a unique complex synchronization configuration.

Remark 7.1. The cases with cycle networks is studied in detail in a follow up paper [4] by Robert Davis and the author where it is established that for cycle networks with *odd* number of oscillators, the facet decomposition scheme always produces the most refined decomposition into primitive subnetworks, and there is an one-to-one correspondence between these primitive subnetworks and the complex synchronization configurations of the original network under the genericity condition. For cycle networks with *even* number of oscillators, however, the facet decomposition scheme alone is not sufficient to produce only primitive subnetworks. A refined decomposition scheme is proposed in the follow up paper [4] that can further decompose cycle networks into only primitive subnetworks.

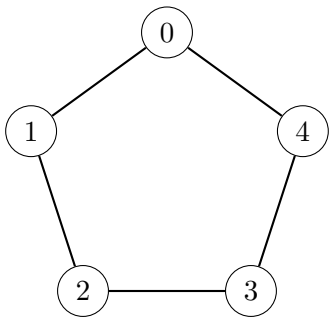

Figure 6. *A cycle of 5 nodes*

7.3. Chordal graphs. We now consider a chordal graph of 4 nodes which consists of a cycle of 4 nodes together with a "chord" edge as shown in Figure 8. Alternatively, such a graph can also be considered as cycle graphs sharing common edges. Figure 9 shows the 12 facet subnetworks. 8 of them are primitive. The remaining are non-primitive but less complicated than the original network.

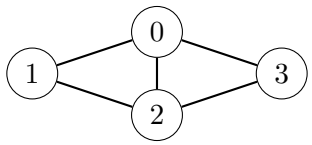

Figure 8. *A chordal graph*

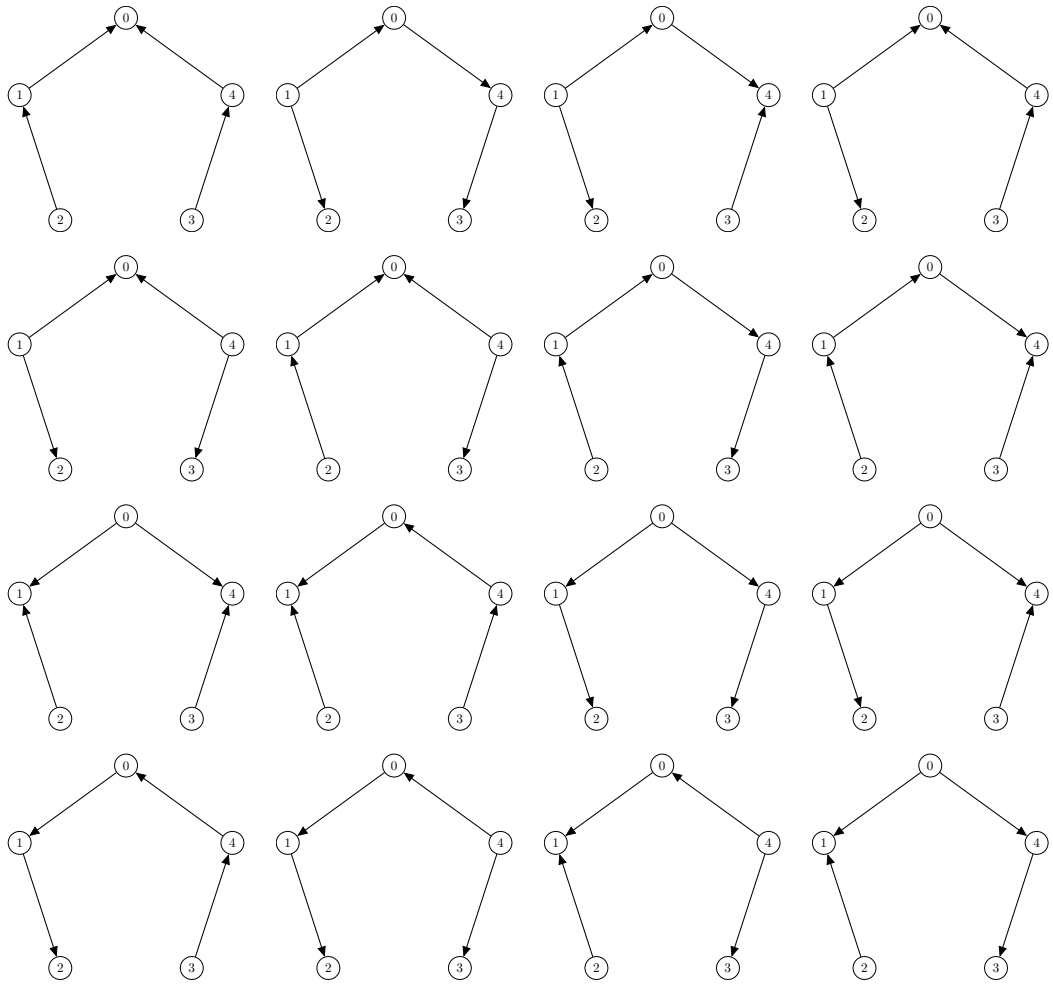

Figure 5. *Facet subnetworks of a tree graph of 5 nodes all of which are primitive*

7.4. Wheel graphs. Finally, we show the facet decomposition scheme for Kuramoto networks whose underlying graph are wheel graphs. A wheel graph is a cycle graph with an additional central node that is directly connected to all other nodes as shown in Figure 10. Since the choice of the reference node in a Kuramoto network is arbitrary, we shall fix the reference node (node 0) to be the central node in our example as this choice produces a decomposition with obvious symmetry. Figure 11 shows all 28 of the facet subnetwork produced from this wheel network. Among them, 12 are primitive. The rest are non-primitive but they are still much simpler than the original Kuramoto network.

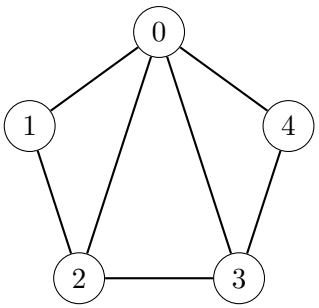

Figure 10. *A wheel of 5 nodes*

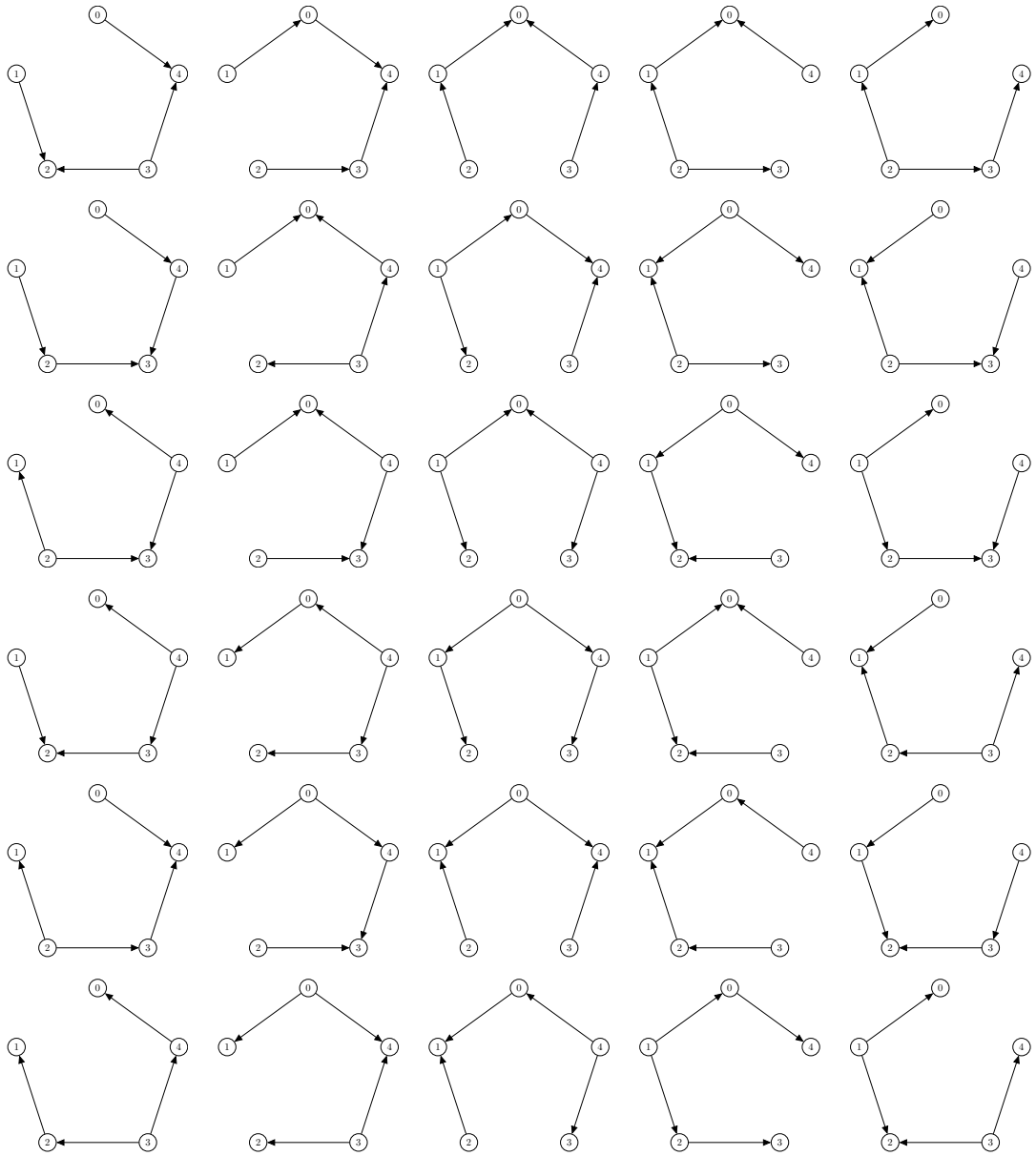

Figure 7. *Facet subnetworks of a cycle graph of 5 nodes all of which are primitive*

8. Concluding remarks. This paper focuses on the study of frequency synchronization configurations in Kuramoto models for networks of coupled oscillators, and it establishes a foundation for a divide-and-conquer approach for analyzing large and complex Kuramoto networks from the view point of algebraic geometry. The main contribution of this paper is a general decomposition scheme for Kuramoto networks that can reduce a complicated Kuramoto network into a collection of simpler directed acyclic subnetworks which are generalized Kuramoto networks that allow one-way interactions among oscillators (c.f. [9]). The problem

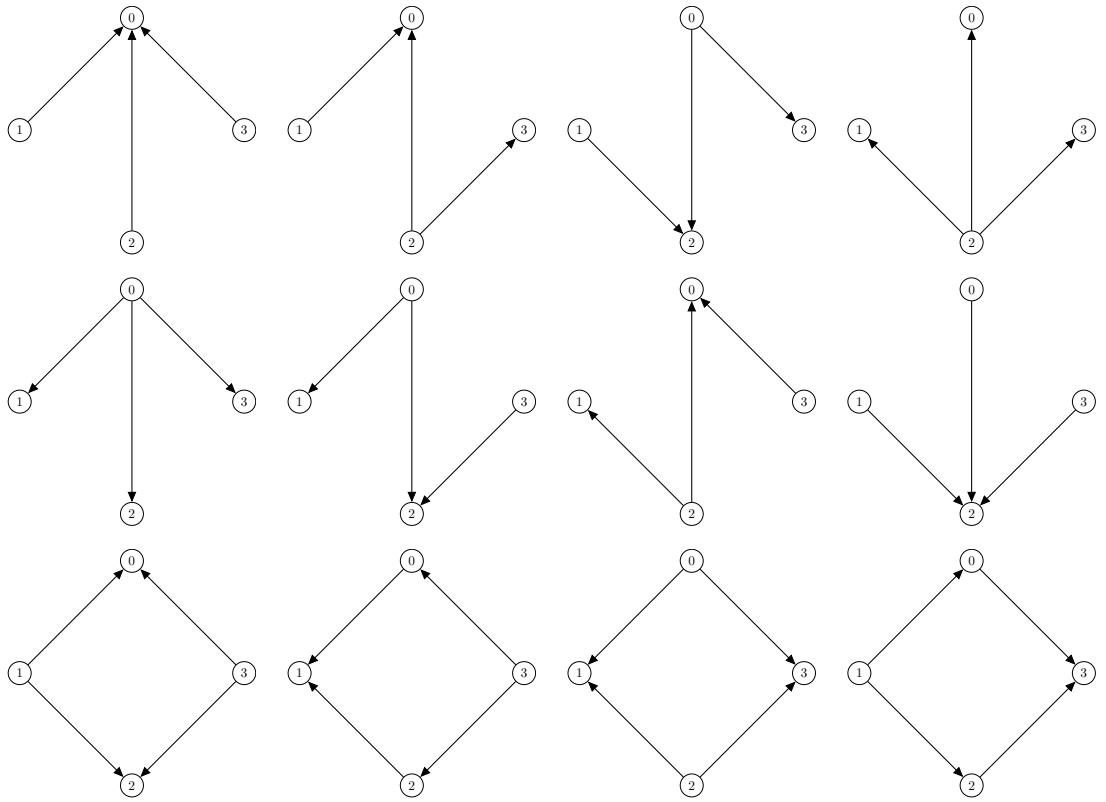

Figure 9. *Facet subnetworks of a chordal graph of 4 nodes*

of finding all possible frequency synchronization configurations is thus reduced to the problem of fully understanding the totality of these much simpler subnetworks.

Starting from a complexified and algebraic re-formulation of the underlying transcendental equations, the proposed framework is created using the geometric information extracted from the "adjacency polytope" of the network which is a polytope that encodes the network topology. This polytope is also the convex hull of the union of the Newton polytopes derived from the algebraic synchronization equations. The subnetworks are then in one-to-one correspondence with the facets (maximal faces) of the adjacency polytope. Since the adjacency polytopes are high symmetric, the facets can be enumerated efficiently. Associated to each of these facet subnetworks is a much simpler generalized synchronization equation, "facet subsystem", which only involve a fraction of the terms from the original algebraic synchronization equations. These subsystems are expected to be easier to solve than the original system. On one end of the spectrum, the facet subsystems associated to primitive subnetworks can be solved in linear time with no additional memory required.

From a computational point of view, the proposed decomposition framework gives rise to a homotopy continuation method: It induces a continuous deformation of the algebraic synchronization system that will degenerate into the collection of simpler facet subsystems. This homotopy method can be viewed as a highly specialized polyhedral homotopy method with

fixed lifting functions (valuation functions). In the case where all subnetworks are primitive, this homotopy construction circumvents two of the main computational bottlenecks of the polyhedral homotopy method:

1. Since the facet subnetworks corresponds to facets of a well known family of polytopes, they can be listed more easily and thereby skips the costly step of "mixed cells computation".
2. The starting system — facet subsystems — can be solved in *linear time* and does not require the costly step of computing Smith Normal Forms or Hermite Normal Forms of exponent matrices.

The examples in the previous section showed that for certain types of networks, some facet subnetworks may not be primitive. The natural next step is to develop algorithms for efficiently refining our facet-based decomposition so that *all* resulting subnetworks are primitive. Recent works showed promising development in this direction. For instance, in a recent follow up paper by Robert Davis and the author, the directed acyclic decomposition scheme proposed here is significantly refined for cycle graphs so that all resulting subnetworks are primitive. This refinement is equivalent to a triangulation process for the facets of the adjacency polytope, but by deriving the explicit formula, the complexity of the refinement step for each facet is only linear in the number of oscillators. The refinement scheme for other types of networks remains an open problem.

Acknowledgments. The author would like to thank Dhagash Mehta for introducing the interesting topic of the Kuramoto model; Daniel Molzahn for helpful discussions on the closely related power-flow equations; and Wuwei Lin for asking the question on whether or not a Kuramoto network can be decomposed into smaller subnetwork in a reasonable way — a question that started this research. The author also greatly benefited from discussions with Robert Davis. Indeed, discussions with Robert Davis produced a significant refinement of the framework developed in this paper for cycle graphs, and this extension becomes a separated follow up paper [4].

REFERENCES

[1] E. L. Allgower, *A survey of homotopy methods for smooth mappings*, in Numerical Solution of Nonlinear Equations, E. L. Allgower, K. Glashoff, and H.-O. Peitgen, eds., no. 878 in Lecture Notes in Mathematics, Springer Berlin Heidelberg, 1981, pp. 1–29, http://link.springer.com/chapter/10.1007/BFb0090675.

[2] J. Baillieul and C. I. Byrnes, *Geometric Critical Point Analysis of Lossless Power System Models*, IEEE Transactions on Circuits and Systems, 29 (1982), pp. 724–737, https://doi.org/10.1109/TCS.1982.1085093.

[3] T. Chen, *Unmixing the mixed volume computation*, arXiv:1703.01684 [math], (2017), http://arxiv.org/abs/1703.01684.

[4] T. Chen and R. Davis, *A toric deformation method for solving Kuramoto equations*, (2018), http://arxiv.org/abs/1810.05690.

[5] T. Chen, R. Davis, and D. Mehta, *Counting Equilibria of the Kuramoto Model Using Birationally Invariant Intersection Index*, SIAM Journal on Applied Algebra and Geometry, 2 (2018), pp. 489–507, https://doi.org/10.1137/17M1145665, https://epubs.siam.org/doi/10.1137/17M1145665.

[6] T. Chen and T.-Y. Li, *Homotopy continuation method for solving systems of nonlinear and polynomial equations*, Commun. Inf. Syst., 15 (2015), pp. 119–307, https://doi.org/10.4310/CIS.2015.v15.n2.a1.

[7] T. Chen and D. Mehta, *On the Network Topology Dependent Solution Count of the Algebraic Load Flow Equations*, IEEE Transactions on Power Systems, 33 (2018), pp. 1451–1460, https://doi.org/10.1109/TPWRS.2017.2724030, http://ieeexplore.ieee.org/document/7971956/.

[8] D. F. Davidenko, *On a new method of numerical solution of systems of nonlinear equations*, in Dokl. Akad. Nauk SSSR, vol. 88, 1953, pp. 601–602.

[9] R. Delabays, P. Jacquod, and F. Dörfler, *The Kuramoto model on directed and signed graphs*, (2018), http://arxiv.org/abs/1807.11410.

[10] F. Dörfler and F. Bullo, *Synchronization in complex networks of phase oscillators: A survey*, Automatica, 50 (2014), pp. 1539–1564, https://doi.org/10.1016/j.automatica.2014.04.012, http://www.sciencedirect.com/science/article/pii/S0005109814001423+.

[11] E. Gawrilow and M. Joswig, *polymake: a Framework for Analyzing Convex Polytopes*, in Polytopes Combinatorics and Computation, Birkhäuser Basel, Basel, 2000, pp. 43–73, https://doi.org/10.1007/978-3-0348-8438-9{_}2, http://link.springer.com/10.1007/978-3-0348-8438-9_2.

[12] B. Huber and B. Sturmfels, *A polyhedral method for solving sparse polynomial systems*, Mathematics of Computation, 64 (1995), pp. 1541–1555, https://doi.org/10.1090/S0025-5718-1995-1297471-4.

[13] A. G. Kouchnirenko, *Polyèdres de Newton et nombres de Milnor*, Inventiones Mathematicae, 32 (1976), pp. 1–31, https://doi.org/10.1007/BF01389769.

[14] Y. Kuramoto, *Self-entrainment of a population of coupled non-linear oscillators*, Lecture Notes in Physics, Springer Berlin Heidelberg, 1975, pp. 420–422, http://link.springer.com/chapter/10.1007/BFb0013365.

[15] Y. Kuramoto, *Chemical Oscillations, Waves, and Turbulence*, Springer Science & Business Media, 12 2012, https://books.google.com/books?id=tcTyCAAAQBAJ.

[16] T.-Y. Li, T. Sauer, and J. A. Yorke, *The cheater's homotopy: an efficient procedure for solving systems of polynomial equations*, SIAM Journal on Numerical Analysis, (1989), pp. 1241–1251.

[17] A. P. Morgan and A. J. Sommese, *Coefficient-parameter polynomial continuation*, Applied Mathematics and Computation, 29 (1989), pp. 123–160, https://doi.org/10.1016/0096-3003(89)90099-4, http://www.sciencedirect.com/science/article/pii/0096300389900994.

[18] A. J. Sommese and C. W. Wampler, *The Numerical Solution of Systems of Polynomials Arising in Engineering and Science*, WORLD SCIENTIFIC, 3 2005, https://doi.org/10.1142/9789812567727, http://ebooks.worldscinet.com/ISBN/9789812567727/9789812567727.html.

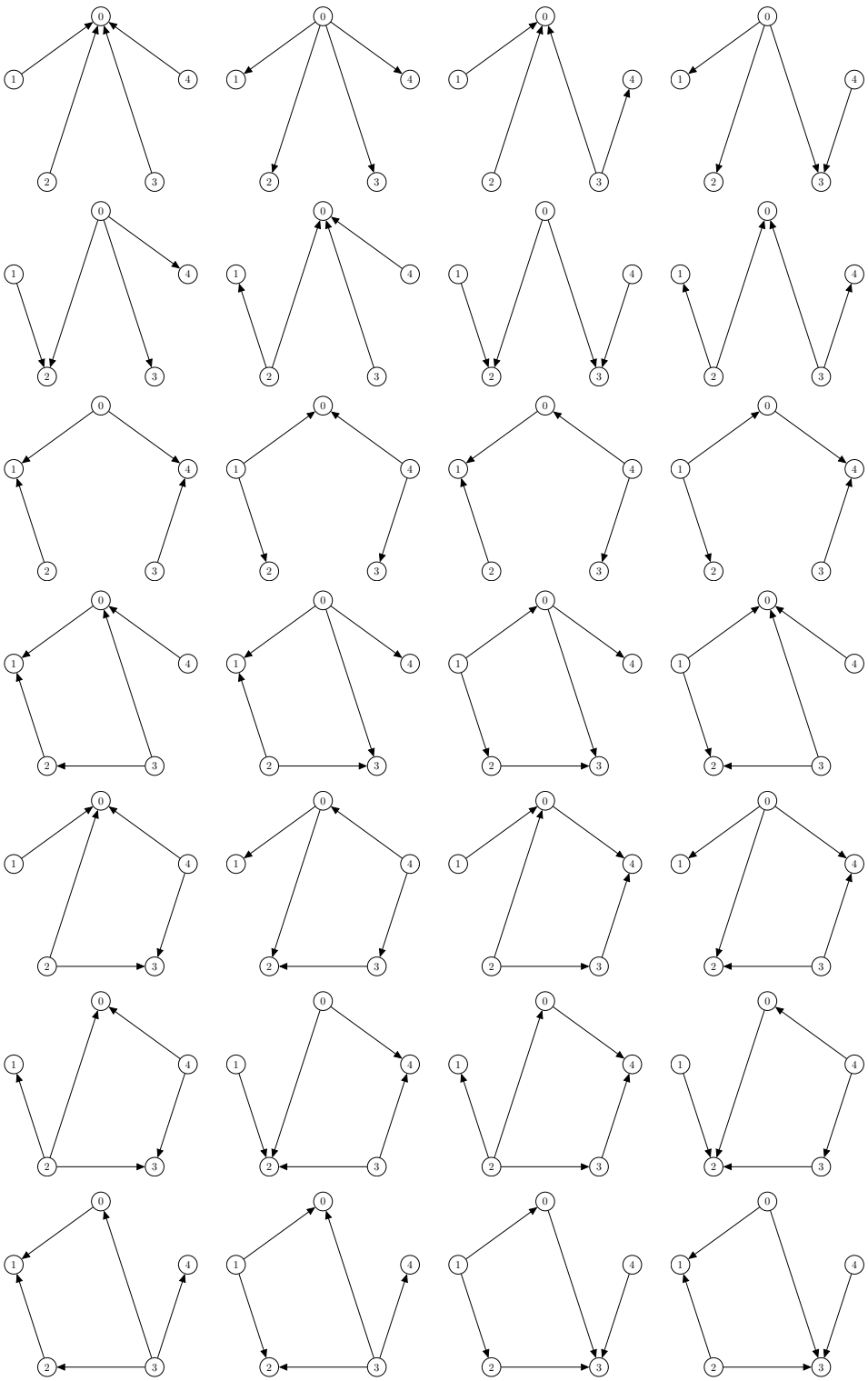

Figure 11. *Facet subnetworks of a wheel graph of 5 nodes*